Organometallics **2001,** *20,* 721−726

Synthesis and Structural Characterization of a Novel Luminescent Tetranuclear Mixed-Metal Platinum(II)−Copper(I) Complex

Vivian Wing-Wah Yam,*,† Ka-Lai Yu, Keith Man-Chung Wong,* and Kung-Kai Cheung

Department of Chemistry, The University of Hong Kong, Pokfulam Road, Hong Kong, People's Republic of China

Received August 15, 2000

A novel tetranuclear mixed-metal platinum(II)−copper(I) complex, $[Pt_2(dppm)_2(C{\equiv}CPh)_4{\cdot}\{Cu(MeCN)\}_2](PF_6)_2$, has been synthesized by the reaction of its precursor complex, $[Pt_2(dppm)_2(C{\equiv}CPh)_4]$, with $[Cu(MeCN)_4]PF_6$. Their crystal structures and luminescence behavior have been determined. Perturbation of the spectroscopic and emission properties has been accomplished by a change in the Pt···Pt distance as well as the π-acceptor ability of the alkynyl unit via Cu(I) coordination.

Introduction

Square-planar platinum(II) complexes have long been known to exhibit metal−metal interactions. A number of these complexes have been shown to exhibit unique spectroscopic properties that are associated with these metal−metal interactions.[1,2] Discrete dinuclear d^8−d^8 metal complexes with well-defined metal−metal distances have also been synthesized and their spectroscopic and luminescence behavior extensively studied.[2,3] The most well-known and well-studied example is the $[Pt_2(pop)_4]^{4-}$ complex, pioneered by Gray, Che, and Roundhill.[2c] Recently, Che[2d,h] and Yam[2d] reported the luminescence properties of a related $[Pt_2(dppm)_2(CN)_4]$, in which the cyanide ligands were believed to play a part in the excited-state properties. To gain further insights into the involvement of ligands with π-acceptor ability in the excited-state properties of these classes of complexes, together with our recent interest in luminescent metal−alkynyl systems,[2g,k,4] we were prompted to investigate the spectroscopic properties of a related face-to-face dinuclear platinum(II) alkynyl complex, $[Pt_2(dppm)_2(C{\equiv}CPh)_4]$, **1**, that was first synthesized by Pringle and Shaw.[5] Utilization of the alkynyl units on **1** as η^2-ligand to encapsulate metal ions such as Cu(I) in a tweezer-like/sandwich fashion has also been achieved to give a highly novel mixed-metal tetranuclear complex, $[Pt_2(dppm)_2(C{\equiv}CPh)_4{\cdot}\{Cu(MeCN)\}_2](PF_6)_2$, **2**. Although a number of reports on the use of metal alkynyl complexes as η^2-ligands to form tweezer-like/sandwich complexes are known,[4e,f,6,7] all of them were confined to the use of mononuclear metal−alkynyl precursors. To the best of our knowledge, this represents the first report on the use of dinuclear metal−alkynyl systems for tweezer-like/sandwich mixed-metal complex formation, in which the metal ions are encapsulated between the alkynyl groups within the same dinuclear molecule. Perturbation of the metal−metal distance as well as the π-acceptor ability of the alkynyl group via Cu(I) encapsulation would provide

---

† Fax: (852)2857-1586. E-mail: wwyam@hku.hk.

(1) Vogler, A.; Kunkely, H. *J. Am. Chem. Soc.* **1981**, *103*, 1559. (b) Lechner, A.; Gliemann, G. *J. Am. Chem. Soc.* **1989**, *111*, 7469. (c) Miskowski, V. M.; Houlding, V. H. *Inorg. Chem.* **1989**, *28*, 1529. (d) Miskowski, V. M.; Houlding, V. H. *Inorg. Chem.* **1991**, *30*, 4446. (e) Wan, K. T.; Che, C. M.; Cho, K. C. *J. Chem. Soc., Dalton Trans.* **1991**, 1077. (f) Houlding, V. H.; Miskowski, V. M. *Coord. Chem. Rev.* **1991**, *111*, 145. (g) Kunkely, H.; Vogler, A. *J. Am. Chem. Soc.* **1990**, *112*, 5625. (h) Zuleta, J. A.; Burbery, M. S.; Eisenberg, R. *Coord. Chem. Rev.* **1990**, *97*, 47.

(2) Filomana Des Remedios, M. A.; Sadler, P. J.; Neidle, S.; Sanderson, M. R.; Subbiah, A. *J. Chem. Soc., Chem. Commun.* **1977**, 62. (b) Zipp, A. P. *Coord. Chem. Rev.* **1988**, *84*, 47. (c) Roundhill, D. M.; Gray, H. B.; Che, C. M. *Acc. Chem. Res.* **1989**, *22*, 55. (d) Che, C. M.; Yam, V. W. W.; Wong, W. T.; Lai, T. F. *Inorg. Chem.* **1989**, *28*, 2908. (e) Smith, D. C.; Gray, H. B. *Coord. Chem. Rev.* **1990**, *100*, 169. (f) Yip, H. K.; Che, C. M.; Zhou, Z. Y.; Mak, T. C. W. *J. Chem. Soc., Chem. Commun.* **1992**, 1369. (g) Yam, V. W. W.; Chan, L. P.; Lai, T. F. *Organometallics* **1993**, *12*, 2197. (h) Yip, H. K.; Lin, H. M.; Cheung, K. K.; Che, C. M.; Wang, Y. *Inorg. Chem.* **1994**, *33*, 1644. (i) Striplin, D. R.; Crosby, G. A. *J. Phys. Chem.* **1995**, *99*, 7977. (j) Yersin, H.; Humbs, W.; Strasser, J. *Coord. Chem. Rev.* **1997**, *159*, 325. (k) Yam, V. W. W.; Yeung, P. K. Y.; Chan, L. P.; Kwok, W. M.; Phillips, D. L.; Yu, K. L.; Wong, R. W. K.; Yan, H.; Meng, Q. J. *Organometallics* **1998**, *17*, 2590.

(3) Mann, K. R.; Gordon, J. G., II; Gray, H. B. *J. Am. Chem. Soc.* **1975**, *97*, 3553. (b) Balch; A. L. *J. Am. Chem. Soc.* **1976**, *98*, 8049. (c) Lewis, N. S.; Mann, K. R.; Gordon, J. G., II; Gray, H. B. *J. Am. Chem. Soc.* **1976**, *98*, 7461. (d) Beveridge, K. A.; Bushell, G. W.; Dixon, K. R.; Eadie, D. T.; Stobart, S. R.; Atwood, J. L.; Zaworotko, M. J. *J. Am. Chem. Soc.* **1982**, *104*, 920. (e) Marshall, J. L.; Hopkins, M. D.; Miskowski, V. M.; Gray, H. B. *Inorg. Chem.* **1992**, *31*, 5034.

(4) Yam, V. W. W. *J. Photochem. Photobiol. A* **1997**, *106*, 75. (b) Yam, V. W. W.; Lo, K. K. W.; Fung, W. K. M.; Wang, C. R. *Coord. Chem. Rev.* **1998**, *171*, 17. (c) Yam, V. W. W.; Lo, K. K. W. *Chem. Soc. Rev.* **1998**, *28*, 323. (d) Yam, V. W. W.; Lo, K. K. W.; Wong, K. M. C. *J. Organomet. Chem.* **1999**, *587*, 3. (e) Yam, V. W. W.; Yu, K. L.; Cheung, K. K. *J. Chem. Soc., Dalton Trans.* **1999**, 2913. (f) Yam, V. W. W.; Chong, S. H. F.; Wong, K. M. C.; Cheung, K. K. *Chem. Commun.* **1999**, 1013.

(5) Pringle, P. G.; Shaw, B. L. *J. Chem. Soc., Chem. Commun.* **1982**, 581. (b) Langrich, C. R.; McEwan, D. M.; Pringle, P. G.; Shaw, B. L. *J. Chem. Soc., Dalton Trans.* **1983**, 2487.

(6) Nast, R. *Coord. Chem. Rev.* **1982**, *47*, 89. (b) Beck, W.; Niemer, B.; Wieser, M. *Angew. Chem., Int. Ed. Engl.* **1993**, *32*, 923. (c) Lang, H.; Köhler, K.; Blau, S. *Coord. Chem. Rev.* **1995**, *143*, 113. (d) Forniés, J.; Lalinde, E. *J. Chem. Soc., Dalton Trans.* **1996**, 2587, and references therein.

(7) Abu Salah, O. M.; Bruce, M. I.; Redhouse, A. D. *J. Chem, Soc., Chem. Commun.* **1974**, 855. (b) Janssen, M. D.; Köhler, K.; Herres, M.; Dedieu, A.; Smeets, W. J. J.; Spek, A. L.; Grove, D. M.; Lang, H.; Koten, G. van *J. Am. Chem. Soc.* **1996**, *118*, 4817. (c) Mihan, S.; Sunkel, K.; Beck, W. *Chem. Eur. J.* **1999**, *5*, 745. (d) Back, S.; Lang, H. *Organometallics* **2000**, *19*, 749.

10.1021/om000713q CCC: $20.00

further insights into the nature of the excited-state origin.

Herein are reported the synthesis of a novel tetranuclear mixed-metal platinum(II)−copper(I) complex, $[Pt_2(dppm)_2(C\equiv CPh)_4\cdot\{Cu(MeCN)\}_2](PF_6)_2$, **2** (dppm = bis(diphenylphosphino)methane), from the complex precursor $[Pt_2(dppm)_2(C\equiv CPh)_4]$, **1**. The crystal structures and spectroscopic properties of **1** and **2** are also described.

Experimental Section

Materials. $[Cu(MeCN)_4]PF_6$[8] was synthesized according to literature procedures. Platinum(II) chloride (99.9%, Strem), dppm (97%, Strem), phenylacetylene (98%, Aldrich), and copper(I) oxide (95%, Strem) were used as received. Dichloromethane for the spectroscopic measurements was washed with concentrated sulfuric acid followed by distillation over CaH_2. All reactions were carried out under strictly anhydrous and anaerobic conditions in a nitrogen atmosphere using standard Schlenk techniques.

Synthesis of Precursor Complex $[Pt_2(dppm)_2(C\equiv CPh)_4]$, 1. This was synthesized according to the reported procedure.[5] X-ray quality yellow crystals of **1** were obtained by recrystallization from CH_2Cl_2/diethyl ether. ^1H NMR (300 MHz, CD_2Cl_2, 298 K, relative to $SiMe_4$): δ 4.60 (m, 4 H, PCH_2P), 6.22 (d, 8 H, phenyl protons *ortho* to $C\equiv C$, $J = 7.2$ Hz), 7.10 (t, 8 H, phenyl protons *meta* to $C\equiv C$, $J = 7.2$ Hz), 7.24 (t, 4 H, phenyl protons *para* to $C\equiv C$, $J = 7.2$ Hz), 7.36 (t, 16 H, phenyl protons *meta* to P, $J = 6.9$ Hz), 7.42 (t, 8 H, phenyl protons *para* to P, $J = 6.9$ Hz), 7.90 (d, 16 H, phenyl protons *ortho* to P, $J = 6.9$ Hz). $^{31}P\{^1H\}$ NMR (202 MHz, CD_2Cl_2, 298 K, relative to 85% H_3PO_4): δ 2.86 (s, $J(Pt-P) = 2795$ Hz). IR (Nujol mull): ν/cm^{-1}($C\equiv C$) 2106 s.

Synthesis of $[Pt_2(dppm)_2(C\equiv CPh)_4\cdot\{Cu(MeCN)\}_2](PF_6)_2$, 2. To a yellow suspension of **1** (80 mg, 0.05 mmol) in dichloromethane (10 mL) was added dropwise $[Cu(MeCN)_4]PF_6$ (38 mg, 0.10 mmol) in acetone solution (10 mL). The reaction mixture immediately turned to a clear greenish-yellow solution and was stirred for 30 min. After removal of solvent under vacuum, a greenish-yellow solid was obtained. Subsequent recrystallization from acetone/*n*-hexane afforded **2** as air-stable greenish-yellow rod-shaped crystals. Yield: 82 mg, 80%. ^1H NMR (300 MHz, CD_2Cl_2, 298 K, relative to $SiMe_4$): δ 1.75 (s, 6 H, CH_3CN), 4.65 (m, 4 H, PCH_2P), 6.20 (d, 8 H, phenyl protons *ortho* to $C\equiv C$, $J = 7.2$ Hz), 7.12 (t, 8 H, phenyl protons *meta* to $C\equiv C$, $J = 7.2$ Hz), 7.24 (t, 4 H, phenyl protons *para* to $C\equiv C$, $J = 7.2$ Hz), 7.36 (t, 16 H, phenyl protons *meta* to P, $J = 6.9$ Hz), 7.45 (t, 8 H, phenyl protons *para* to P, $J = 6.9$ Hz), 7.96 (d, 16 H, phenyl protons *ortho* to P, $J = 6.9$ Hz). $^{31}P\{^1H\}$ NMR (202 MHz, CD_2Cl_2, 298 K, relative to 85% H_3PO_4): δ 5.24 (s, $J(Pt-P) = 2540$ Hz). IR (Nujol mull): ν/cm^{-1}($C\equiv C$) 2024 w. FT-Raman (solid): ν/cm^{-1}($C\equiv C$) 2026 s. Positive ESI-MS: ion clusters at m/z 1627 $\{M - Cu - 2MeCN\}^+$, 845 $\{M - 2MeCN\}^{2+}$. Anal. Calcd for **2** ($- CH_3CN$) $C_{84}H_{67}NF_{12}P_6Cu_2Pt_2$: C, 49.90; H, 3.32; N 0.69. Found: C, 49.79; H, 3.33; N 0.63.

Physical Measurements and Instrumentation. UV−visible spectra were obtained on a Hewlett-Packard 8452A diode array spectrophotometer, IR spectra as Nujol mulls on a Bio-Rad FTS-7 Fourier transform infrared spectrophotometer (4000−400 cm^{-1}), FT-Raman spectra on a Bio-Rad FT Raman spectrometer, and positive ESI mass spectra on a Finnigan LCQ mass spectrometer. ^1H NMR spectra, with chemical shifts reported relative to tetramethylsilane, and ^{31}P NMR spectra with chemical shifts relative to 85% H_3PO_4 were recorded on Bruker DPX-300 and Bruker DPX-500 NMR spectrometers, respectively. Elemental analyses were performed on a Carlo Erba 1106 elemental analyzer at the Institute of Chemistry in Beijing, Chinese Academy of Sciences.

Steady-state emission and excitation spectra at room temperature and at 77 K were obtained on a Spex Fluorolog-2 model F111 fluorescence spectrophotometer with or without Corning filters. The 77 K solid-state emission and excitation spectra were recorded with solid samples loaded in a quartz tube inside a quartz-walled optical Dewar flask filled with liquid nitrogen. For solution emission and excitation spectral studies, the solutions were prepared in a 10 mL Pyrex bulb connected to a sidearm 1 cm quartz cuvette and sealed from the atmosphere by a Rotaflo HP6/6 quick-release Teflon stopper. The solutions were degassed with no fewer than four freeze−pump−thaw cycles. Emission-lifetime measurements were performed using a conventional laser system. The excitation source was the 355 nm output (third harmonic) of a Spectra-Physics Quanta-Ray Q-switched GCR-150-10 pulsed Nd:YAG laser. Luminescence decay signals were recorded on a Tektronix model TDS620A digital oscilloscope and analyzed using a program for exponential fits. Time-resolved emission spectra were recorded on an Oriel Instruments intensified charge-coupled device (ICCD) detector (Model DH520) and were analyzed using the InstaSpec V software. The excitation source is the same laser system as that used for lifetime measurement. The emission signal was collected by an optical fiber and dispersed onto the CCD detector with an Oriel MultiSpec 115 imaging spectrograph (Model 77480). A Stanford Research Systems (SRS) delay generator (Model DG 535) was used to produce the transistor−transistor logic (TTL) pulse needed to operate the intensifier gating electronics in the detector head. The external trigger input of the delay generator was connected to the laser's prepulse trigger output. The delay generator was controlled via an IBM AT APIB (IEEE 488) card interfaced with an IBM-compatible Pentium personal computer to allow the InstaSpec V software to send commands to control the width and delay of the TTL pulse. The system was operated at −15 °C by the single-stage system in order to reduce the dark current signal.

Crystal Structure Determination. Crystal data for $[C_{82}H_{64}P_4Pt_2\cdot 5CH_2Cl_2]$, $1\cdot 5CH_2Cl_2$: fw = 1988.15, monoclinic, space group $P2_1/n$ (No. 14), $a = 13.502(2)$ Å, $b = 21.201(3)$ Å, $c = 14.863(2)$ Å, $\beta = 105.60(2)°$, $V = 4097(1)$ Å^3, $Z = 2$, $D_c = 1.611$ g cm^{-3}, μ(Mo Kα) = 38.45 cm^{-1}, $F(000) = 1964$, $T = 301$ K. A yellow crystal of dimensions 0.20 × 0.10 × 0.10 mm inside a glass capillary was used for data collection at 28 °C on a MAR diffractometer with a 300 mm image plate detector using graphite-monochromatized Mo Kα radiation ($\lambda = 0.71073$ Å). Data collection was made with 2.5° oscillation (60 images) at 120 mm distance and 540 s exposure. The images were interpreted and intensities integrated using the program DENZO.[9a] A total of 7328 unique reflections were obtained from a total of 32 537 measured reflections ($R_{int} = 0.050$). A total of 5682 reflections with $I > 3\sigma(I)$ were considered observed and used in the structural analysis. These reflections were in the range h: 0 to 12; k: 0 to 42; and l: −25 to 25 with $2\theta_{max} = 51.1°$. The space group was uniquely determined based on systematic absences, and the structure was solved by direct methods (SIR92[9b]) and expanded by the Fourier method. Refinement was by full-matrix least-squares using the software package TeXsan[9c] on a Silicon Graphics Indy computer.

---

(8) Kubas, G. J. *Inorg. Synth.* **1979**, *19*, 90.

(9) *DENZO*: In *The HKL Manual−A description of programs DENZO, XDISPLAYF, and SCALEPACK*; written by Gewirth, D. with the coorperation of the program authors Otwinowski, Z., Minor, W. Yale University: New Haven, CT, 1995. (b) *SIR92*: Altomare, A.; Cascarano, M.; Giacovazzo, C.; Guagliardi, A.; Burla, M. C.; Polidori, G.; Camalli, M. *J. Appl. Crystallogr.* **1994**, *27*, 435. (c) *TeXsan*: *Crystal Structure Analysis Package*; Molecular Structure Corporation: The Woodlands, TX, 1985, 1992. (d) *PATTY*: Beurskens, P. T.; Admiraal, G.; Beurskens, G.; Bosman, W. P.; Garcia-Granda, S.; Gould, R. O.; Smits J. M. M.; Smykalla, C. *The DIRDIF program system*; Technical Report of the Crystallography Laboratory; University of Nijmegen, The Netherlands, 1992.

Table 1. Crystal and Structure Determination Data

	1	**2**
formula	$C_{82}H_{64}P_4Pt_2{\cdot}5CH_2Cl_2$	$C_{86}H_{70}N_2F_{12}P_6Cu_2Pt_2$
fw	1988.15	2062.61
T, °C	28	28
a, Å	13.502(2)	11.144(2)
b, Å	21.201(3)	34.978(3)
c, Å	14.863(2)	21.557(3)
β, deg	105.60(2)	94.16(2)
V, Å^3	4097(1)	8380(1)
cryst syst	monoclinic	monoclinic
space group	$P2_1/n$	*C*2/*c* (No. 15)
Z	2	4
F(000)	1964	4048
D_c, g cm^{-3}	1.611	1.635
crystal color/shape	yellow crystal	yellow crystal
cryst dimens, mm	0.20 × 0.10 × 0.10	0.40 × 0.15 × 0.07
λ, Å (graphite monochromated, Mo Kα)	0.71073	0.71073
μ, cm^{-1}	38.45	40.01
collection range	$2\theta_{max}$= 51.1°; ±*h*, *k*, *l*	$2\theta_{max}$= 51.1°; ±*h*, *k*, *l*
data collection mode	2.5° oscillation (60 images) × 120 mm distance × 540 s exposure	2° oscillation (90 images) × 100 mm distance × 600 s exposure
no. of data collected	32 537	41 515
no. of unique data	7328	7288
R_{int}	0.050	0.067
no. of data used in refinement, *m*	5682 ($I > 3\sigma(I)$)	4975 ($I > 3\sigma(I)$)
no. of params refined, *p*	469	271
R	0.033[a]	0.042[b]
R_w	0.049	0.064
S	1.50	2.51
maximum shift, (shift/error)$_{max}$	0.04 except for C atoms of the solvent molecules	0.05 except for the disordered C atoms
residual extrema in final diff map, e Å^{-3}	+1.35, −1.03	+1.29, −1.96

[a] $w = 4F_o^2/\sigma^2(F_o^2)$ where $\sigma^2(F_o^2) = [\sigma^2(I) + (0.040F_o^2)^2]$ with $I > 3\sigma(I)$. [b] $w = 4F_o^2/\sigma^2(F_o^2)$ where $\sigma^2(F_o^2) = [\sigma^2(I) + (0.029F_o^2)^2]$ with $I > 3\sigma(I)$.

One crystallographic asymmetric unit consists of half of one molecule, two CH_2Cl_2 solvent molecules in general positions, and half a molecule of CH_2Cl_2 with the C atom in general position having half-occupation and one Cl atom and the disordered C atom generated by symmetry, having coordinates at $1-x$, $-y$, $-z$. In the least-squares refinement, all 52 non-H atoms were refined anisotropically, and 36 H atoms at calculated positions with thermal parameters equal to 1.3 times that of the attached C atoms were not refined. The H atoms of the disordered C atom were not included. Convergence for 469 variable parameters by least-squares refinement on *F* with $w = 4F_o^2/\sigma^2(F_o^2)$, where $\sigma^2(F_o^2) = [\sigma^2(I) + (0.040F_o^2)^2]$ for 5682 reflections with $I > 3\sigma(I)$, was reached at $R = 0.033$ and $wR = 0.049$ with a goodness-of-fit of 1.50. $(\Delta/\sigma)_{max} = 0.04$ except for the C atoms of the solvent molecules. The final difference Fourier map was featureless, with maximum positive and negative peaks of 1.35 and 1.03 e Å^{-3}, respectively.

Crystal data for [$C_{86}H_{70}N_2F_6P_6Cu_2Pt_2$], 2: fw = 2062.61, monoclinic, space group *C*2/*c* (No. 15), $a = 11.144(2)$ Å, $b = 34.978(3)$ Å, $c = 21.557(3)$ Å, $\beta = 94.16(2)°$, $V = 8380(1)$ Å^3, $Z = 4$, $D_c = 1.635$ g cm^{-3}, μ(Mo Kα) = 40.01 cm^{-1}, *F*(000) = 4048, *T* = 301 K. A yellow crystal of dimensions 0.40 × 0.15 × 0.07 mm inside a glass capillary was used for data collection at 28 °C on a MAR diffractometer with a 300 mm image plate detector using graphite-monochromatized Mo Kα radiation (λ = 0.71073 Å). Data collection was made with 2° oscillation (90 images) at 100 mm distance and 600 s exposure. The images were interpreted and intensities integrated using the program DENZO.[9a] A total of 7288 unique reflections were obtained from a total of 41 515 measured reflections ($R_{int} = 0.067$). A total of 4975 reflections with $I > 3\sigma(I)$ were considered observed and used in the structural analysis. These reflections were in the range *h*: 0 to 12; *k*: 0 to 42; and *l*: −25 to 25 with $2\theta_{max} = 51.1°$. The space group was determined based on systematic absences and on a statistical analysis of intensity distribution, the successful refinement of structure solved was by Patterson methods and expanded by Fourier methods (PATTY[9d]), and refinement was by full-matrix least-squares using the software package TeXsan[9c] on a Silicon Graphics Indy computer. A crystallographic asymmetric unit consists of half of one formula unit with the copper and the acetonitrile atoms at special positions. The phenyl ring of the acetylenic group C(12) and C(13) was disordered, and each of the six C atoms was placed at two positions with equal occupancies. In the least-squares refinement, only the six Pt, Cu, and P atoms were refined anisotropically, the other 59 non-H were refined isotropically, and 33 H atoms at calculated positions with thermal parameters equal to 1.3 times that of the attached C atoms were not refined. The H atoms of the disordered phenyl ring were not included in the calculation. Convergence for 271 variable parameters by least-squares refinement on *F* with $w = 4F_o^2/\sigma^2(F_o^2)$, where $\sigma^2(F_o^2) = [\sigma^2(I) + (0.029F_o^2)^2]$ for 4975 reflections with $I > 3\sigma(I)$, was reached at $R = 0.042$ and $wR = 0.064$ with a goodness-of-fit of 2.51. $(\Delta/\sigma)_{max} = 0.05$ except for the disordered C atoms. The final difference Fourier map was featureless, with maximum positive and negative peaks of 1.29 and 1.96 e Å^{-3}, respectively. Crystal and structure determination data as well as the selected bond distances and bond angles of **1** and **2** are collected in Tables 1 and 2, respectively.

Results and Discussion

Complex **1** is not very soluble in common organic solvents but only dissolves slowly in dichloromethane, while **2** is very soluble in acetone, dichloromethane, and acetonitrile. In the preparation of **2**, the reaction mixture immediately turns to a greenish-yellow solution

Table 2. Selected Bond Distances (Å) and Angles (deg) with Estimated Standard Deviations in Parentheses

[$Pt_2(\mu$-dppm$)_2(C{\equiv}CPh)_4$] (1)

Bond Distances (Å)

Pt(1)−P(1)	2.304(1)	C(9)−C(10)	1.185(8)
Pt(1)−P(2)	2.299(1)	P(1)−C(29)	1.839(5)
Pt(1)−C(1)	2.004(6)	P(2)−C(29)	1.840(6)
Pt(1)−C(9)	2.014(5)	Pt(1)−Pt(1)*	3.437(1)
C(1)−C(2)	1.194(8)		

Bond Angles (deg)

P(1)−Pt(1)−P(2)	173.87(5)	Pt(1)−C(1)−C(2)	177.0(5)
P(1)−Pt(1)−C(1)	91.9(2)	Pt(1)−C(9)−C(10)	169.9(5)
P(1)−Pt(1)−C(9)	90.4(2)	C(1)−C(2)−C(3)	174.2(7)
P(2)−Pt(1)−C(1)	93.0(2)	C(9)−C(10)−C(11)	178.4(6)
P(2)−Pt(1)−C(9)	85.4(2)	P(1)−C(29)−P(2)	121.2(3)
C(1)−Pt(1)−C(9)	169.5(2)		

[$Pt_2(dppm)_2(C{\equiv}CPh)_4\cdot\{Cu(MeCN)\}_2](PF_6)_2$ (2)

Bond Distances (Å)

Pt(1)−P(1)	2.313(3)	Pt(1)−Pt(1)*	3.0124(9)
Pt(1)−P(2)	2.319(3)	Cu(1)−C(1)	2.12(1)
Pt(1)−C(1)	2.02(1)	Cu(2)−C(12)	2.10(4)
Pt(1)−C(12)	2.00(1)	Cu(2)−C(13)	2.09(1)
C(1)−C(2)	1.20(2)	Cu(1)−N(1)	1.96(2)
C(12)−C(13)	1.21(2)	Cu(2)−N(2)	2.01(4)
P(1)−C(34)	1.82(1)	N(1)−C(10)	1.13(3)
P(2)−C(34)	1.84(1)	N(2)−C(20)	0.93(7)

Bond Angles (deg)

P(1)−Pt(1)−P(2)	176.7(1)	Pt(1)−C(1)−C(2)	164.8(10)
P(1)−Pt(1)−C(1)	92.8(3)	Pt(1)−C(12)−C(13)	165(1)
P(1)−Pt(1)−C(12)	86.2(3)	C(1)−C(2)−C(3)	167(1)
P(2)−Pt(1)−C(1)	89.8(3)	C(12)−C(13)−C(14)	161(1)
P(2)−Pt(1)−C(12)	91.0(3)	N(1)−Cu(1)−C(1)	128.2(3)
C(1)−Pt(1)−C(12)	174.4(4)	N(2)−Cu(2)−C(12)	128.5(3)

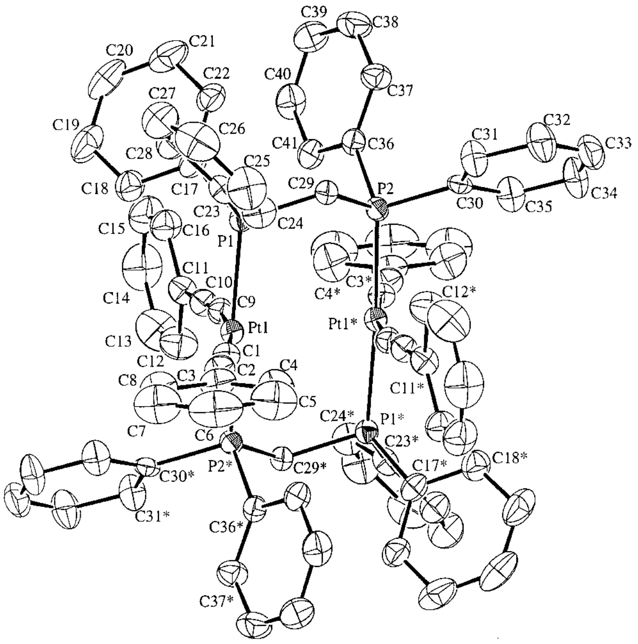

Figure 1. Perspective drawing of **1** with atomic numbering scheme. The H atoms have been omitted for clarity. Thermal ellipsoids are shown at 40% probability level.

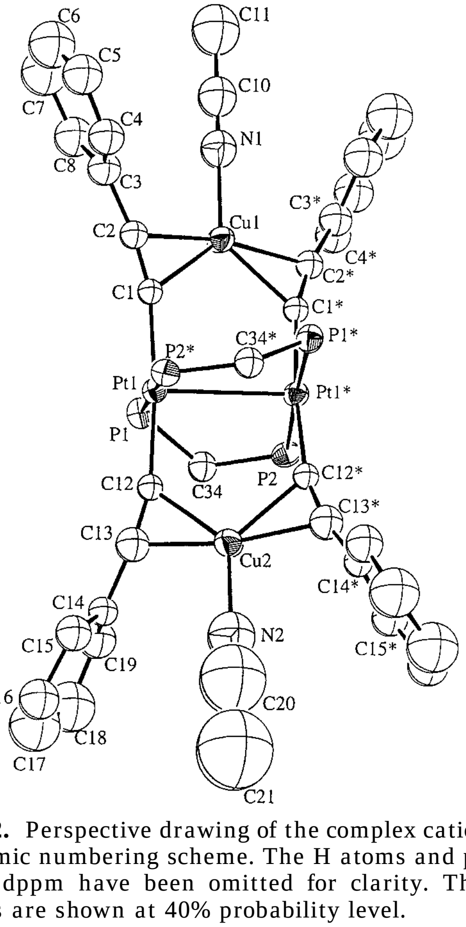

Figure 2. Perspective drawing of the complex cation of **2** with atomic numbering scheme. The H atoms and phenyl rings of dppm have been omitted for clarity. Thermal ellipsoids are shown at 40% probability level.

upon addition of [$Cu(MeCN)_4]PF_6$ to a pale yellow suspension of **1**, indicating a fast reaction rate. The identity of **2** has been established by ^1H NMR, ^{31}P NMR, ESI-MS, IR, FT-Raman, and satisfactory elemental analyses. Recrystallization of **1** from CH_2Cl_2/diethyl ether afforded X-ray quality crystals. The crystal structures of **1** and **2** have been determined by X-ray crystallography.

Although the positive ESI-MS data and elemental analyses show the loss of acetonitrile molecule(s) attached to the copper(I) centers from **2**, ^1H NMR spectroscopy in CD_2Cl_2 confirms that the structure of **2** remains intact in solution under ambient conditions with two acetonitrile molecules attached to the two copper(I) ions. The $^{31}P\{^1H\}$ NMR spectrum of **2** shows a singlet with platinum satellites at δ 5.24 ppm with a Pt−P coupling constant of 2540 Hz, typical of a *trans* arrangement of the P−Pt−P unit. The downfield shift of the ^{31}P resonance signal in **2** relative to **1** [2.83 ppm with J(Pt−P) of 2795 Hz] is consistent with the presence of the more electron-deficient platinum centers in **2** as a result of the electron donation from the alkynyl groups to the copper(I) ions.

Figures 1 and 2 depict the perspective drawings of **1** and the complex cation of **2** with atomic numbering, respectively. Both of them adopt a face-to-face arrangement in which each platinum atom is coordinated to two *trans* alkynyl ligands [C−Pt−C, 169.5(2)° **1**; 174.4(4)° **2**] and two *trans* bridging dppm [P−Pt−P, 173.87(5)° **1**; 176.7(1)° **2**] to form an eight-membered ring. The platinum atoms exhibit distorted square-planar coordination [P−Pt−C, 85.4(2)−93.0(2)° **1**; 86.2(3)−92.8(3)° **2**] and are eclipsed with each other. It is noteworthy that the Pt···Pt distance for **2** [3.0124(9) Å] is significantly shorter than that for **1** [3.437(1) Å]. The Pt···Pt distance of **1** is comparable to that of the related [$Pt_2(dppm)_2(CN)_4$] [Pt···Pt 3.301(1) Å],[2d] while that of **2** is slightly longer than that for $K_4[Pt_2(pop)_4]$ [2.925(1) Å],[2a] indicative of the presence of metal−metal interactions. The shortening of the Pt···Pt distance in **2** relative to

Table 3. Photophysical Data for Complex 1 and 2

complex	absorption[a] λ/nm (ϵ_{max}/dm^3 mol^{-1} cm^{-1})	emission medium (T/K)	emission λ_{em}/nm (τ_o/μs)
1	270 (56 810), 330 (28 890), 370 (25 540)	CH_2Cl_2 (298)	620 (<0.1)
		solid (298)	580 {615}[c] (<0.1)
		solid (77)	607 (6.0 ± 0.6)
		glass[a] (77)	460 (3.4 ± 0.3), 545[d] (8.2 ± 0.8)
2	372 (33 160), 418 (18 350)	CH_2Cl_2 (298)	625 (0.22 ± 0.02)
		solid (298)	495, 610 (2.2 ± 0.2)
		solid (77)	490 (4.1 ± 0.4), 634 (6.1 ± 0.6)
		glass[b] (77)	476 (2.0 ± 0.2), 590[e] (8.9 ± 0.9)

[a] In CH_2Cl_2. [b] In EtOH/MeOH (4:1 v/v), emission maxima are recorded by time-resolved emission measurement. [c] In crystal form before rigorous drying. [d] Vibronic-structured with vibrational progressional spacings of 2220 cm^{-1}. [e] Vibronic-structured with vibrational progressional spacings of 2024 cm^{-1}.

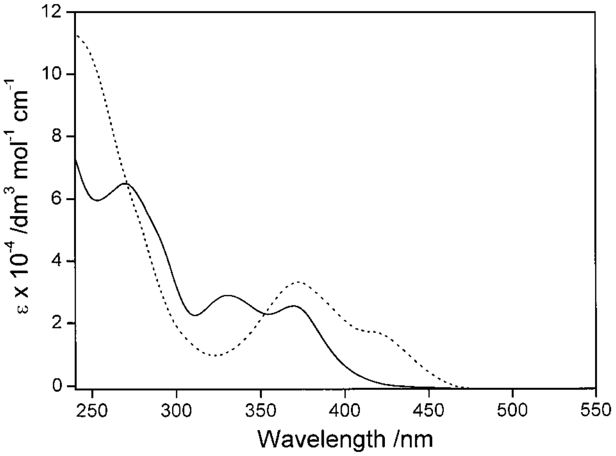

Figure 3. Electronic absorption spectra of **1** (—) and **2** (- - -) in CH_2Cl_2 solution at 298 K.

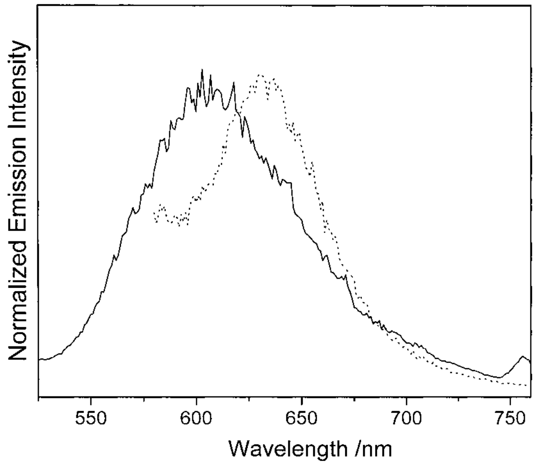

Figure 4. Emission spectra of **1** (—) and **2** (- - -) in the solid state at 77 K.

that of **1** has been ascribed to the encapsulation of copper(I) ion by two adjacent alkynyl ligands, which pulls the platinum atoms into close proximity as a result of the reduced donor strength of the alkynyl ligands upon copper(I) coordination. The reduced electron density on the platinum centers in **2** would tend to pull the metal centers closer for metal−metal interactions to occur. The slightly longer $C\equiv C$ bond distances for **2** [1.21(2) and 1.20(2) Å] than **1** [1.194(8) and 1.185(8) Å] is indicative of a weakening of the $C\equiv C$ bond upon π-coordination to copper(I), in line with the observation of a lower $C\equiv C$ stretching frequency [2024(w) cm^{-1} **2**; 2106(s) cm^{-1} **1**] in the IR spectroscopy. In **2**, each copper(I) ion coordinates to two alkynyl groups and one acetonitrile molecule in a trigonal-planar geometry. Similar geometry has also been commonly observed in related d^{10} metal-containing organometallic compounds.[7]

The electronic absorption data of **1** and **2** are summarized in Table 3, and their electronic absorption spectra are shown in Figure 3. The electronic absorption spectrum of **1** shows absorption bands at 330 and 370 nm, while that of **2** occurs at 372 and 418 nm. With reference to previous spectroscopic work on $[Pt_2(dppm)_2(CN)_4]$,[2d] the intense band at ca. 370 nm that is absent in the monomeric $[Pt(dppm)_2(C\equiv CR)_2]$,[2g,10,11] in which only an absorption band at 345 nm assignable to a mixed metal-to-alkynyl MLCT/intraligand IL [$\pi \rightarrow \pi^*$-($C\equiv CPh$)] transition is observed, is assigned as a metal-centered $^1[(d_\sigma{}^*)^2] \rightarrow {}^1[(d_\sigma{}^*)^1(p_\sigma)^1]$ transition with substantial mixing of a metal−metal bond-to-ligand charge-transfer MMLCT $^1[d_\sigma{}^* \rightarrow p_\sigma/\pi^*(C\equiv CPh)]$ character, where $d_\sigma{}^*$ and p_σ denote the antibonding combination of $d_{z^2}(Pt)-d_{z^2}(Pt)$ interaction and bonding combination of $p_z(Pt)-p_z(Pt)$ interaction, respectively, taking the Pt···Pt direction as the *z*-axis. Similar assignments have also been suggested for $[Pt(dppm)_2(CN)_4]$,[2d] $[Rh_2(dppm)_2(CNR)_4]^{2+}$,[3a] and the binuclear Pt(II) μ-alkenylidene complexes.[12] The red shift of the absorption band in **2** relative to **1** is also consistent with such an assignment since a narrowing of the HOMO−LUMO energy gap would occur upon shortening of the Pt···Pt distance from **1** to **2**. Moreover, the increased π-accepting ability of the $PhC\equiv C$ groups upon π-coordination to the Cu^I ion, which could be viewed as a Lewis acid, would also account for the red shift in absorption energy in **2** relative to **1**, as a result of the lowering of the $\pi^*(PhC\equiv C)$ orbital energy.

Upon photoexcitation at λ > 350 nm, **1** and **2** exhibit strong emission both in the solid state and in fluid solution at room temperature and 77 K. Their emission data are collected in Table 3. The emission spectra of **1** and **2** in the solid state at 77 K are shown in Figure 4. In the solid state and glass state at 77 K, **2** displays two emission bands, and this phenomenon can also be observed for **1** in glass state at 77 K. Because of the

---

(10) Yip, H. K.; Lin, H. M.; Wang, Y.; Che, C. M. *J. Chem. Soc., Dalton Trans.* **1993**, 2939.

(11) Masai, H.; Sonogashira, K.; Hagihara, N. *Bull. Chem. Soc. Jpn.* **1971**, *44*, 2226.

(12) Sacksteder, L. A.; Baralt, E.; DeGraff, B. A.; Lukehart, C. M.; Demas, J. N. *Inorg. Chem.* **1991**, *30*, 3955. (b) Baralt, E.; Boudreaux, E. A.; Demas, J. N.; Lenhert, P. G.; Lukehart, C. M.; McPhail, A. T.; McPhail, D. R.; Myers, J. B., Jr.; Sacksteder, L. A.; True, W. R. *Organometallics* **1989**, *8*, 2417.

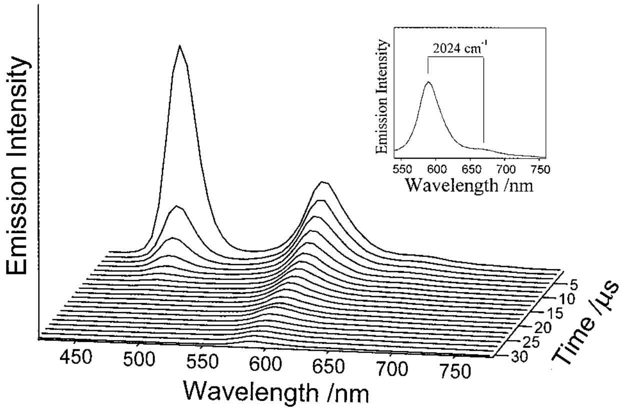

Figure 5. Time-resolved emission spectra of **2** in EtOH/MeOH glass (4:1 v/v) at 77 K.

relatively large energy difference between the two bands ($\Delta E > 3000$ cm^{-1}) and their difference in excited-state lifetimes, they are suggested to be of different origins. Figure 5 depicts the 3D-plot of the time-resolved emission spectra of **2** in EtOH/MeOH (4:1 v/v) glass at 77 K. In view of the relatively long lifetime in the microsecond range, the higher energy emission bands (460−495 nm) observed in **1** and **2** are unlikely to be derived from singlet excited states and are tentatively assigned as intraligand phosphorescence of the bridging diphosphine ligands. The low-energy emission bands at ca. 540−600 nm in 77 K glass, which are vibronically structured with vibrational progressional spacings of ca. 2000−2200 cm^{-1} that are typical of the ν(C≡C) stretch in the ground state, are suggestive of an involvement of the PhC≡C moiety in the emissive state. With reference to previous spectroscopic works on related d^8−d^8 dinuclear systems,[2d,g,h,k,12] the low-energy emission band is ascribed to phosphorescence derived from the ^{3}MMLCT state. The lower emission energy of **2** than **1** is in line with the reduced Pt···Pt separation in **2**, which gives rise to a larger dσ−dσ* splitting and hence an increase in the dσ* orbital energy, as well as a decrease of the π*(PhC≡C) orbital energy in **2** upon coordination of Cu(I) ions. Similar findings have also been observed in the electronic absorption studies. The smaller vibrational progressional spacings in **2** (2024 cm^{-1}) than **1** (2220 cm^{-1}) are also consistent with the reduced bond strength of the C≡C bond upon π-coordination to the Cu(I) ions in **2**.

Acknowledgment. V.W.-W.Y. acknowledges financial support from the Research Grants Council and The University of Hong Kong and the receipt of a Croucher Foundation Senior Research Fellowship from the Croucher Foundation; K.-L.Y., the receipt of a postgraduate studentship administered by The University of Hong Kong; and K.M.-C.W., the receipt of a University Postdoctoral Fellowship, also administered by The University of Hong Kong.

Supporting Information Available: Tables of atomic coordinates, thermal parameters, and a full list of bond distances and angles for **1** and **2** are deposited as Supporting Information. This material is available free of charge via the Internet at http://pubs.acs.org.

OM000713Q